IOP Publishing Journal of Physics G: Nuclear and Particle Physics

J. Phys. G: Nucl. Part. Phys. **47** (2020) 055005 (23pp) https://doi.org/10.1088/1361-6471/ab7ff9

Probing model-independent limits on $W^+W^-\gamma$ triple gauge boson vertex at the LHeC and the FCC-he

A Gutiérrez-Rodríguez[1,2], M Köksal[3,6], A A Billur[4] and M A Hernández-Ruíz[5]

[1] Facultad de Física, Universidad Autónoma de Zacatecas Apartado, Postal C-580, 98060 Zacatecas, México
[2] Unidad Académica de Estudios Nucleares, Universidad Autónoma de Zacatecas, 98060 Zacatecas, México
[3] Department of Optical Engineering, Sivas Cumhuriyet University, 58140, Sivas, Turkey
[4] Department of Physics, Sivas Cumhuriyet University, 58140, Sivas, Turkey
[5] Unidad Académica de Ciencias Químicas, Universidad Autónoma de Zacatecas Apartado, Postal C-585, 98060 Zacatecas, México

E-mail: alexgu@fisica.uaz.edu.mx, mkoksal@cumhuriyet.edu.tr, abillur@cumhuriyet.edu.tr and mahernan@uaz.edu.mx

Received 13 October 2019, revised 9 March 2020
Accepted for publication 13 March 2020
Published 9 April 2020

Abstract

We study the cross-section of production of a single W^- boson in association with a neutrino through the process $e^-p \to e^-\gamma^* p \to \nu_e W^- p$. Additionally, we obtain limits on the anomalous couplings $\Delta\kappa_\gamma$ and λ_γ of the $W^+W^-\gamma$ vertex at the Large Hadron electron Collider (LHeC) and the future circular collider hadron-electron (FCC-he). The impact of the polarized beam due to the electron is also analyzed. Our best limits for $\Delta\kappa_\gamma$ and λ_γ at the 95% C.L. are: $\Delta\kappa_\gamma = \pm 0.0017$, $\lambda_\gamma = \pm 0.0053$ (unpolarized electron beam) and $\Delta\kappa_\gamma = \pm 0.0013$, $\lambda_\gamma = \pm 0.0046$ (polarized electron beam) identifying the W^- boson through the hadronic decay channel. In addition, the $e^-\gamma^* \to \nu_e W^-$ collision is one of the clean, pure and simple processes to probe the $W^+W^-\gamma$ coupling without the complications of QCD backgrounds.

Keywords: models beyond the standard model, W bosons, triple gauge boson couplings

(Some figures may appear in colour only in the online journal)

[6] Author to whom any correspondence should be addressed.

1. Introduction

The standard model (SM) [1–3] of elementary particle physics based on the gauge group $SU(2)_L \times U(1)_Y$, describes the electroweak interactions as being mediated by the γ-photon, the Z-boson and the $W^{\pm}$-bosons.

The $W^{\pm}$-bosons are among the heaviest particles known of the SM. Although the properties of the $W^{\pm}$-boson have been studied for many years, measuring its mass, as well as its anomalous couplings with high precision remains a great challenge and an important objective to prove the unification of the electromagnetic and weak interactions in the SM. High precision measurement of the properties of these bosons has made these particles one of the most attractive particles for new physics research.

It is worth mentioning that it is very important to measure the masses of the $W^{\pm}$-bosons, as well as its anomalous couplings, as accurately as possible to better understand the Higgs boson, refine the SM and test its global consistency.

As we mentioned above, an outstanding feature of the SM is the self coupling of the gauge bosons, that is $WW\gamma$, WWZ, $WZ\gamma$, $W\gamma\gamma$, $WW\gamma\gamma$, $WWZ\gamma$, $WWZZ$ and $WWWW$. It is thus of great importance to test the anomalous triple-gauge-boson couplings (aTGC) and anomalous quartic-gauge-boson couplings (aQGC). Furthermore, the aTGC and aQGC are a very important element in the search for the new physics beyond the SM (BSM), because any difference of the measured value with respect to the predicted could unveil new phenomena other than the SM. For these and other reasons, is very important to studying the gauge bosons self-interactions. In this paper we focus on measurements of the charged triple gauge boson couplings, $\Delta\kappa_\gamma$ and λ_γ i.e. those of form $WW\gamma$. These aTGC have been bounded by measurements of gauge boson pair production WW performed at the LEP, the Tevatron and the LHC. Limits on these couplings have been obtained from hadron collider experiments UA2 experiment at the CERN [4], CDF and D0 experiments at the Fermilab Tevatron [5–10]. CLEO Collaboration obtain measurements on the anomalous $WW\gamma$ coupling of the process $B(b \to s\gamma)$ [11]. In the case of lepton colliders experiments, the ALEP, DELPHI, L3 and OPAL experiments at the LEP [12], as well as the TESLA [13] experiments have also obtained bounds on anomalous couplings $WW\gamma$. More recently, the ATLAS and CMS collaborations at the Large Hadron Collider (LHC) of CERN have obtained limits on the aTGC $\Delta\kappa_\gamma$ and λ_γ, respectively.

The physics program of the future linear colliders such as the international linear collider (ILC) [19] and the compact linear collider CLIC [20], as well as of the future lepton-hadron circular colliders (FCC) at CERN, that is the LHeC [21–24] and the FCC-he [25], operating as e^+e^- and e^-p colliders, also contemplate the study of anomalous couplings $\Delta\kappa_\gamma$ and λ_γ operating in the collisions $e^-\gamma$, $\gamma\gamma$, $e^-\gamma^*$, $\gamma^*\gamma^*$, γp and $\gamma^* p$ modes.

The $\nu_e W^-$ production at the e^-p colliders contains a lot of information on the existence of trilinear self-couplings among $W^+W^-\gamma$ gauge bosons. These couplings are a consequence of the non-Abelian gauge structure of the SM, predict the existence of the triple couplings $W^+W^-\gamma$ [1–3]. As we mentioned above, the $W^+W^-\gamma$ triple gauge boson vertex is accessible at the present and future colliders such as the LHC, LHeC, FCC-he and the CLIC at CERN for the post LHC era, as well as at the ILC, CEPC and FCC-ee.

Under these arguments, in this paper, we study and present our results on the cross-section of the process $e^-p \to e^-\gamma^* p \to \nu_e W^- p$. In addition, we obtain model-independent limits on the anomalous electromagnetic couplings $\Delta\kappa_\gamma$ and λ_γ of the $W^+W^-\gamma$ vertex for the high-energies of the center-of mass energies $\sqrt{s} = 1.30, 1.98, 7.07, 10$ TeV and high-luminosities $\mathcal{L} = 10 - 1000$ fb^{-1} of the LHeC and the FCC-he [21–23, 25, 28, 29]. Additionally, we consider unpolarized and polarized electron beams, as well as the systematic

Table 1. Updated summary on the comparison of experimental and phenomenological bounds at 95% C.L. on the aTGC $\Delta\kappa_\gamma$ and λ_γ from the present and future colliders.

Model	$\Delta\kappa_\gamma$	λ_γ	C. L.	References
SM	0	0		[1–3]
Experimental limit	$\Delta\kappa_\gamma$	λ_γ	*C. L.*	*References*
ATLAS Collaboration	[−0.061, 0.064]	[−0.013, 0.013]	95%	[14]
CMS Collaboration	[−0.044, 0.063]	[−0.011, 0.011]	95%	[15]
CDF Collaboration	[−0.158, 0.255]	[−0.034, 0.042]	95%	[9]
D0 Collaboration	[−0.158, 0.255]	[−0.034, 0.042]	95%	[10]
ALEP, DELPHI, L3, OPAL	[−0.099, 0.066]	[−0.059, 0.017]	95%	[12]
Phenomenological limit	$\Delta\kappa_\gamma$	λ_γ	*C. L.*	*References*
LHC	[−0.0058, 0.0058]	[−0.0011, 0.0011]	95%	[16]
HL-LHC	[−0.014, 0.014]	[−0.0033, 0.0033]	95%	[16]
LHeC	[−0.0016, 0.0024]	[−0.0040, 0.0043]	95%	[17]
FCC-he	[−0.00069, 0.000 69]	[−0.0099, 0.0054]	95%	[18]
CEPC	[−0.00045, 0.000 45]	[−0.00033, 0.000 33]	95%	[16]
ILC	[−0.00037, 0.000 37]	[−0.00051, 0.000 51]	95%	[26]
CLIC	[−0.00007, 0.000 07]	[−0.00004, 0.000 04]	95%	[27]

uncertainties $\delta_{\rm sys} = 0\%, 1\%, 5\%, 10\%$ [30, 31] and leptonic and hadronic decays of the W-boson.

A updated summary of experimental and phenomenological limits at 95% C.L. on the aTGC $\Delta\kappa_\gamma$ and λ_γ from the present and future colliders is given in table 1. See [32–46] for other limits on the anomalous $W^+W^-\gamma$ couplings in different contexts.

This work is organized as follows: in section 2 we give an overview of the operators in the effective Lagrangian. In section 3 we derive limits on the anomalous couplings $\Delta\kappa_\gamma$ and λ_γ at the LHeC and the FCC-he. In section 4 we present our conclusions.

2. Effective field theory (EFT) approach to non-standard *WWγ* couplings

An appropriate approach and model-independent for describing possible new physics effects is based on EFT approach. In this approach, all the heavy degrees of freedom are integrated out to obtain effective interactions between the SM particles. This is justified since the related observables have so far not shown any significant deviation from the SM predictions.

We start from the EFT approach to study the process $e^-p \to e^-\gamma^* p \to \nu_e W^- p$, as well as to determine limits on the aTGC $\Delta\kappa_\gamma$ and λ_γ. In this regard, our starting point is the Lagrangian of the EFT of the SM which can be expanded as:

$$\mathcal{L} = \mathcal{L}_{\rm SM} + \sum_i \frac{C_i}{\Lambda^2}\mathcal{O}_i + ... + \text{h.c}\,., \tag{1}$$

where the coefficients C_i are dimensionless and parameterize the strength with which the new physics couples to the SM particles, while Λ is some characteristic heavy scale of the system. The $\mathcal{O}_i$ are the dimension-6 operators constructed with the light fields.

To define our notation we quote here the operators relevant for $e^- p \to e^- \gamma^* p \to \nu_e W^- p$ with anomalous couplings $\Delta\kappa_\gamma$ and λ_γ, which can be written as:

$$\mathcal{L} = \frac{1}{\Lambda^2}[C_W \mathcal{O}_W + C_B \mathcal{O}_B + C_{WWW}\mathcal{O}_{WWW} + \text{h.c.}], \tag{2}$$

where the three independent dimension-6 operators $\mathcal{O}_W$, $\mathcal{O}_B$ and $\mathcal{O}_{WWW}$ that C and P conserving are specified as follows:

$$\mathcal{O}_W = (D_\mu \Phi)^\dagger \hat{W}^{\mu\nu}(D_\nu \Phi), \tag{3}$$

$$\mathcal{O}_B = (D_\mu \Phi)^\dagger \hat{B}^{\mu\nu}(D_\nu \Phi), \tag{4}$$

$$\mathcal{O}_{WWW} = Tr[\hat{W}^{\mu\nu}\hat{W}^{\rho}_{\nu}\hat{W}_{\mu\rho}]. \tag{5}$$

Here D_μ and Φ are the covariant derivative and the Higgs doublet field, while $\hat{B}_{\mu\nu}$ and $\hat{W}_{\mu\nu}$ are the field strength tensors, respectively. It is appropriate to mention that in the decoupling limit $\Lambda \to \infty$ and the coefficients C_W/Λ^2, C_B/Λ^2, and C_{WWW}/Λ^2 of equation (2) are zero.

With all these elements given above, the EFT approach to anomalous couplings $\Delta\kappa_\gamma$ and λ_γ is based on the Lagrangian [33, 47]:

$$\mathcal{L}_{WW\gamma} = -ig_{WW\gamma}\left[g_1^\gamma (W^\dagger_{\mu\nu}W^\mu A^\nu - W^{\mu\nu}W^\dagger_\mu A_\nu) + \kappa_\gamma W^\dagger_\mu W_\nu A^{\mu\nu} + \frac{\lambda_\gamma}{M_W^2}W^\dagger_{\rho\mu}W^\mu_\nu A^{\nu\rho}\right], \tag{6}$$

where all the terms of equation (6) C and P conserving and $W^\pm_{\mu\nu} = \partial_\mu W^\pm_\nu - \partial_\nu W^\pm_\mu$, while the overall coupling constant is defined as $g_{WW\gamma} = e$. On the other hand, the electromagnetic gauge invariance implies that $g_1^\gamma = 1$, while $\kappa_\gamma = 1$ and $\lambda_\lambda = 0$ in the SM.

The EFT approach using here allows us calculate the parameters $\Delta\kappa_\gamma$ and λ_γ in terms of the coefficients of the three dimension-6 operators given by equation (2). These coefficients are related to the aTGC $\Delta\kappa_\gamma$ and λ_γ [34, 48, 49] as:

$$\kappa_\gamma = 1 + \Delta\kappa_\gamma, \tag{7}$$

where specifically $\Delta\kappa_\gamma$ is given by:

$$\Delta\kappa_\gamma = C_W + C_B, \tag{8}$$

$$\lambda_\gamma = C_{WWW}. \tag{9}$$

On the other hand, the vertex function approach is the momentum-space analog of the EFT approach given by equation (6). In this context, the vertex function approach which C and P conserving and that is consistent with gauge and Lorentz invariance of the SM, is parameterized [33] as:

$$\Gamma^{WW\gamma}_{\mu\nu\rho} = e[g_{\mu\nu}(p_1 - p_2)_\rho + g_{\nu\rho}(p_2 - p_3)_\mu + g_{\rho\mu}(p_3 - p_1)_\nu + \Delta\kappa_\gamma(g_{\rho\mu}p_{3\nu} - g_{\nu\rho}p_{3\mu}) + \frac{\lambda_\gamma}{M_W^2}(p_{1\rho}p_{2\mu}p_{3\nu} - p_{1\nu}p_{2\rho}p_{3\mu} - g_{\mu\nu}(p_2 \cdot p_3 p_{1\rho} - p_3 \cdot p_1 p_{2\rho}) - g_{\nu\rho}(p_3 \cdot p_1 p_{2\mu} - p_1 \cdot p_2 p_{3\mu}) - g_{\mu\rho}(p_1 \cdot p_2 p_{3\nu} - p_2 \cdot p_3 p_{1\nu})]. \tag{10}$$

In this equation the first three terms corresponds to the SM couplings, while the terms with $\Delta\kappa_\gamma$ and λ_γ correspond to the contribution of the aTGC.

3. Cross-section of the process $e^- p \to e^- \gamma^* p \to \nu_e W^- p$ and limits on the anomalous couplings $\Delta\kappa_\gamma$ and λ_γ

3.1. Cross-section of the process $e^- p \to e^- \gamma^* p \to \nu_e W^- p$ at the LHeC and the FCC-he

The LHeC and the FCC-he are proposed, designed and planned colliders to carry out $e^- p$ collisions at center-of-mass energies $\sqrt{s} = 1.30$, 1.97, 7.07 and 10 TeV, that is to say with a four main stage research region [21–23, 25, 28, 29]. The $e^- p$ colliders can also be operated as $e^-\gamma^*$, $\gamma^* p$ and $\gamma^*\gamma$ colliders. This enables the investigation of the $e\gamma^*$ interactions where the emitted quasi-real photon γ^* is scattered with small angles from the beam pipe of e^- [50–55]. Since these photons have a low virtuality, they are almost on the mass shell. These processes can be described by the equivalent photon approximation (EPA) [53, 56, 57], using the Weizsacker–Williams approximation. The EPA has a lot of advantages such as providing the skill to reach crude numerical predictions via simple formulae. Furthermore, it may principally ease the experimental analysis because it enables one to directly achieve a rough cross-section for $e^-\gamma^* \to X$ process via the examination of the main process $e^- p \to e^- X p$ where X represents objects produced in the final state. The production of high mass objects is particularly interesting at the $e^- p$ colliders and the production rate of massive objects is limited by the photon luminosity at high invariant mass while the $e\gamma^*$ process at the e^- p colliders arises from quasi-real photon emitted from the incoming beams. In many studies, new physics investigations are examined by using the EPA [73, 58–72, 74–78].

Another very important element in our study corresponds to the impact of the polarization of the electron beam. About this, in the baseline LHeC and FCC-he design, the electron beam can be polarized up to $\pm 80\%$. By selecting different beam polarizations it is possible to enhance or suppress different physical processes. In the particular case of the process $e^- p \to e^-\gamma^* p \to \nu_e W^- p$, the chiral nature of the weak coupling to fermions can result in significant possible enhancements in $\nu_e W^-$ production. Starting from this, the polarized e^- beam combined with the clean experimental environment provided by the LHeC and the FCC-he will allow to improve strongly the potential of searches for the $W^+W^-\gamma$ triple gauge boson vertex. With these arguments, we consider polarized electron beam in our study. The expression for the total cross-section for an arbitrary degree of longitudinal e^- beam polarization is given by [79]:

$$\sigma_{e_r^-} = \sigma_{e_0^-} \cdot (1 - P_{e_r^-}),\ \sigma_{e_l^-} + \sigma_{e_r^-} = 2\sigma_{e_0^-}, \tag{11}$$

where $\sigma_{e_r^-}$, $\sigma_{e_l^-}$ and $\sigma_{e_0^-}$ represent the right, left and without electron beam polarization, respectively and P_{e^-} is the polarization degree of the electron.

The schematic diagram corresponding to the process $e^- p \to e^-\gamma^* p \to \nu_e W^- p$ is given in figure 1. While the representative leading order Feynman diagrams for the subprocess $\gamma^* e^- \to \nu_e W^-$ are depicted in figure 2. We based our calculations on electron-photon fluxes

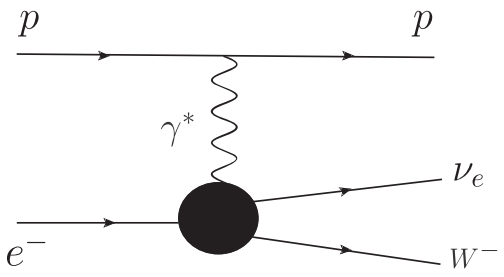

Figure 1. A schematic diagram for the process $e^-p \to e^-\gamma^* p \to \nu_e W^- p$.

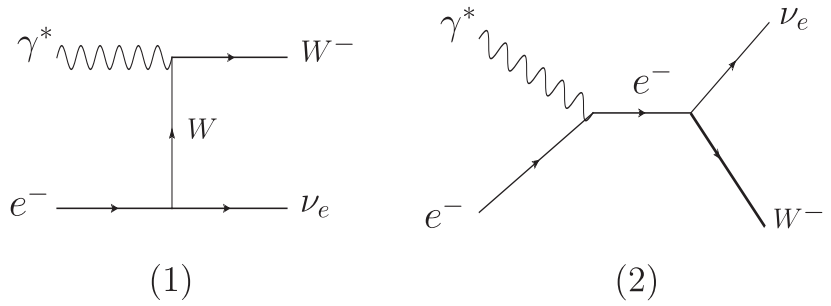

Figure 2. Feynman diagrams contributing to the subprocess $\gamma^* e^- \to \nu_e W^-$.

through the subprocess $e^-\gamma^* \to \nu_e W^-$. In addition, it is evident the contribution of elastic process with an intact proton in the final state.

Finally, the total cross-section is obtained by folding the elementary cross-section with the photon distribution function:

$$\sigma(e^-p \to e^-\gamma^* p \to \nu_e W^- p) = \int f_{\gamma^*}(x)\hat{\sigma}(e^-\gamma^* \to \nu_e W^-)\mathrm{d}x, \tag{12}$$

where $\hat{\sigma}(e^-\gamma^* \to \nu_e W^-)$ is the cross-section for the reaction $e^-\gamma^* \to \nu_e W^-$, and the distribution function $f_{\gamma^*}(x)$ of the EPA photons which are emitted by protons is given by [53, 80]:

$$f_{\gamma^*}(x) = \frac{\alpha}{\pi E_p}\{[1-x][\varphi\left(\frac{Q^2_{\mathrm{max}}}{Q^2_0}\right) - \varphi\left(\frac{Q^2_{\mathrm{min}}}{Q^2_0}\right)], \tag{13}$$

where $x = E_\gamma/E_p$ and Q^2_{max} is the maximum virtuality of the photon. For our calculations, we use $Q^2_{\mathrm{max}} = 2\ \mathrm{GeV}^2$. The minimum value of the Q^2_{min} is:

$$Q^2_{\mathrm{min}} = \frac{m_p^2 x^2}{1-x}. \tag{14}$$

From equation (13), the function φ is given by:

$$\varphi(\theta) = (1 + ay)\left[-\mathrm{In}(1 + \frac{1}{\theta}) + \sum_{k=1}^{3}\frac{1}{k(1+\theta)^k}\right] + \frac{y(1-b)}{4\theta(1+\theta)^3} + c(1 + \frac{y}{4})\left[\mathrm{In}\left(\frac{1-b+\theta}{1+\theta}\right) + \sum_{k=1}^{3}\frac{b^k}{k(1+\theta)^k}\right], \tag{15}$$

where explicitly y, a, b and c are as follows:

$$y = \frac{x^2}{(1-x)}, \tag{16}$$

$$a = \frac{1+\mu_p^2}{4} + \frac{4m_p^2}{Q_0^2} \approx 7.16, \tag{17}$$

$$b = 1 - \frac{4m_p^2}{Q_0^2} \approx -3.96, \tag{18}$$

$$c = \frac{\mu_p^2 - 1}{b^4} \approx 0.028. \tag{19}$$

In order to perform our calculations in an efficient way, we used a numerical method. The numerical integration is performed using the CalcHEP packages [80].

The present LHeC and the FCC-he are planned to generate e^-p collisions at energies from 1.30 to 10 TeV [42, 65]. The LHeC is a suggested deep inelastic electron–nucleon scattering machine which has been planned to collide electrons with an energy from 60 GeV to possibly 140 GeV, with protons with an energy of 7 TeV. In addition, the FCC-he is designed for collider electrons with an energy from 250 to 500 GeV, with protons with an energy of 50 TeV. The LHeC and the FCC-he physics programs will enable fundamentally new insights beyond the capabilities of the LHC for the anomalous coupling $W^+W^-\gamma$. In addition, the flexibility and large accessible energy range provides a wide range of possibilities to measure the new physics using very different approaches.

It is appropriate to mention that the phenomenological investigations at e^-p colliders generally contain deep inelastic scattering reactions where the colliding proton dissociates into partons. Although inelastic processes have been more examined in literature, exclusive γ^*p and $\gamma^*\gamma^*$ processes have been less probed. Exclusive processes can be distinguished from completely inelastic processes due to some experimental signatures. First, after the photon emission in γ^*p collisions, proton is scattered with a small angle and escape detection from the central detectors. This gives rise to a missing energy signature called the forward large-rapidity gap, in the corresponding forward region of the central detector. Also, another experimental signature can be implemented by forward particle tagging. These detectors are to tag the protons with some energy fraction loss. Deflected protons and their energy loss will be detected by the forward detectors mentioned above but other products in the final state will go to the central detector. Finally, operation of forward detectors in conjunction with central detectors with precise timing, can efficiently reduce backgrounds. In this context, LHeC Collaboration has a program of forward physics with extra detectors located in a region between a few tens up to several hundreds of meters from the interaction point [21].

The high-luminosity and the low backgrounds of QCD give access to the process $e^-p \to e^-\gamma^*p \to \nu_e W^-p$ at all energies. Furthermore, the clean experimental environment

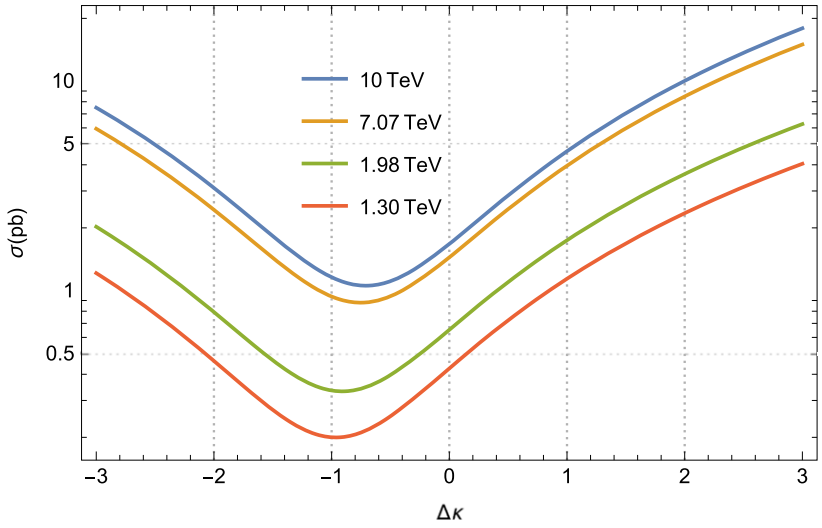

Figure 3. The total cross sections of the process $e^-p \to e^-\gamma^* p \to \nu_e W^- p$ as a function of $\Delta\kappa_\gamma$ for center-of-mass energies of $\sqrt{s} = 1.30, 1.98, 7.07, 10$ TeV at the LHeC and the FCC-he.

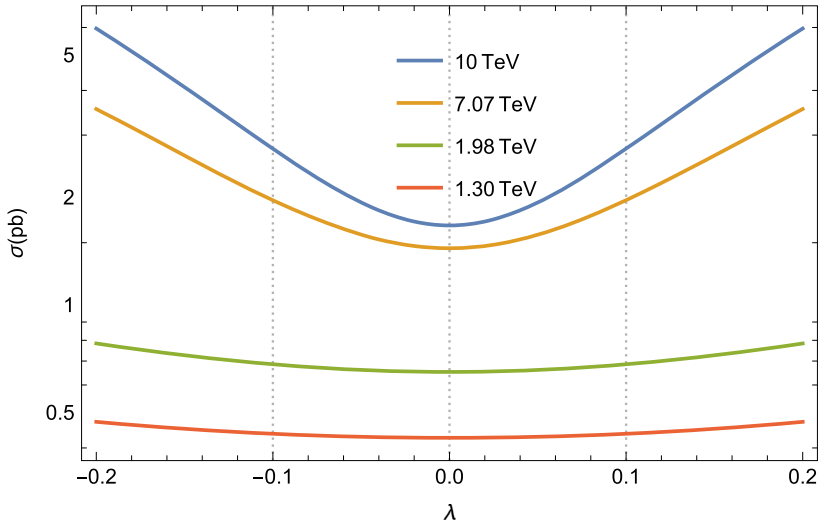

Figure 4. Same as in figure 3, but for λ_γ.

and the good knowledge of the initial state allow precise measurements of the cross-section of the $\nu_e W^-$ signal, as well as of $\Delta\kappa_\gamma$ and λ_γ, respectively.

Figure 3 shows the total cross-sections of the process $e^-p \to e^-\gamma^* p \to \nu_e W^- p$ as a function of $\Delta\kappa_\gamma$ for center-of-mass energies of $\sqrt{s} = 1.30, 1.98, 7.07, 10$ TeV at the LHeC and the FCC-he. The mechanism $e^-p \to e^-\gamma^* p \to \nu_e W^- p$ is dominant at $\sqrt{s} = 10$ TeV reaching a cross-section of 20 pb. A similar study on the cross-sections of the process $e^-p \to e^-\gamma^* p \to \nu_e W^- p$ as a function of λ_γ is presented in figure 4. In this case, the cross-

section obtained is of 5 pb at center-of-mass energy of $\sqrt{s} = 10$ TeV. In general, this process can be identified at all the energy stages of the LHeC and the FCC-he.

From figure 3 (and similarly in figure 7), in the case of 1.30 and 1.98 TeV where the center-of-mass energies are relatively low, there is an asymmetry of the cross-section values relative to the negative and positive values of the anomalous couplings $\Delta\kappa_\gamma$ and λ_γ. This is due to the cross terms of the anomalous couplings with SM terms It is observed that this asymmetry decreased significantly due to the reduction of the effect of the SM in increasing center-of-mass energies.

3.2. Limits on the anomalous couplings $\Delta\kappa_\gamma$ and λ_γ at the LHeC and the FCC-he

One of the main purposes of this paper is to determine the best measurements of the anomalous couplings $\Delta\kappa_\gamma$ and λ_γ at the LHeC and the FCC-he. To carry out this purpose, we adopted a χ^2 analysis. The χ^2 function for our fit is defined as similar [81–84]:

$$\chi^2(\Delta\kappa_\gamma, \lambda_\gamma) = \left(\frac{\sigma_{\rm SM} - \sigma_{\rm BSM}(\sqrt{s}, \Delta\kappa_\gamma, \lambda_\gamma)}{\sigma_{\rm SM}\sqrt{(\delta_{\rm st})^2 + (\delta_{\rm sys})^2}} \right)^2, \tag{20}$$

where $\sigma_{\rm BSM}(\sqrt{s}, \Delta\kappa_\gamma, \lambda_\gamma)$ and $\sigma_{\rm SM}$ are the cross-section in the presence of beyond SM interactions and in the SM, respectively. $\delta_{\rm st} = \frac{1}{\sqrt{N_{\rm SM}}}$ is the statistical error and $\delta_{\rm sys}$ is the systematic error. The number of events is given by $N_{\rm SM} = \mathcal{L}_{\rm int} \times \sigma_{\rm SM} \times {\rm BR}(W^\pm \to qq', l\nu_l)$, where $\mathcal{L}_{\rm int}$ is the integrated luminosity and $l = e^-, \mu$. We values assume for the systematic uncertainties of $\delta_{\rm sys} = 0\%, 1\%, 5\%$ and 10% [30, 31]. For single W^- production at the LHeC and the FCC-he we classify their decay products according to the decomposition of W^-. In this paper, we consider that the W^- boson decay leptonically or hadronically for the signal. Thus, we assume that the branching ratios for W^- decays are: ${\rm BR}(W^- \to qq') = 0.674$ for hadronic decays and ${\rm BR}(W^- \to l\nu) = 0.213$ for light leptonic decays.

Systematic uncertainties play a key role in the measurement of physical quantities such as the anomalous $\Delta\kappa_\gamma$ and λ_γ couplings. Systematic uncertainties, on the other hand, arise from uncertainties associated with the nature of the measurement apparatus, assumptions made by the experimenter, or the model used to make inferences based on the observed data. Common systematic uncertainties include uncertainties that arise from the calibration of the measurement device, the probability of detection of a given type of interaction often called the acceptance of the detector, and parameters of the model used. In this sense, an important aspect of our study is the incorporation of theoretical uncertainties as there may be several experimental and systematic uncertainty sources when identifying to the *W*-boson. The most common sources of systematic uncertainties are: trigger efficiency, selection efficiency, background, luminosity, parton distribution functions (PDFs).

It may be assumed that the LHeC and the FCC-he will be built in the coming years and substantially improves the precision achieved in the hadron electron ring accelerator analysis, reducing the systematic uncertainties for the trigger efficiency, selection efficiency, background, luminosity, PDF for the LHeC and even more for the FCC-he.

We examine in figures 5 and 6 the impact of center-of-mass energies $\sqrt{s} =$ 1.30, 1.98, 7.07, 10 TeV and the luminosities $\mathcal{L} =$ 10, 50, 100, 500, 1000 fb^{-1} on the anomalous couplings $\Delta\kappa_\gamma$ and λ_γ. The expected measurement for both $\Delta\kappa_\gamma$ and λ_γ is 10^{-2} for 7.07, 10 TeV and 100, 500, 1000 fb^{-1}, respectively. For other energy stages of the LHeC, the expected measurements on $\Delta\kappa_\gamma$ and λ_γ are an order of magnitude weaker. However, for all the energy

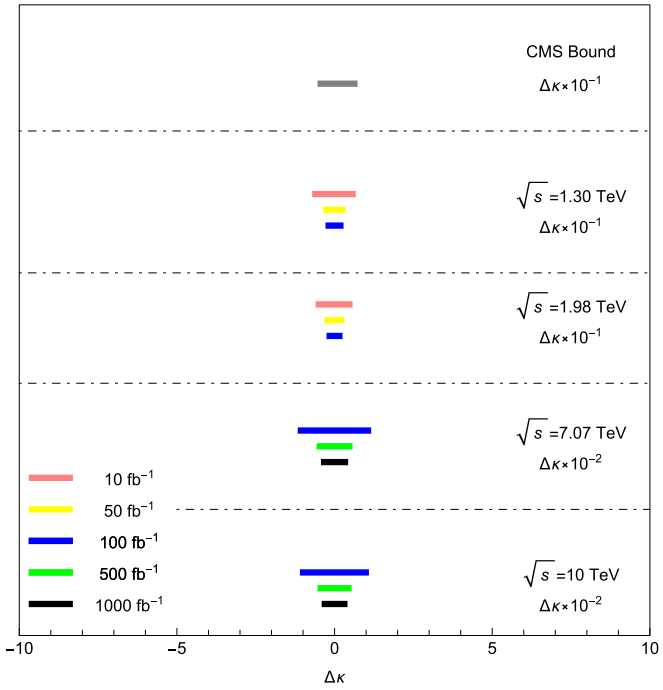

Figure 5. Comparison of precisions at the LHeC and the FCC-he to the anomalous coupling $\Delta\kappa_\gamma$ for center-of-mass energies $\sqrt{s} = 1.30, 1.98, 1.07, 10$ TeV and luminosities $\mathcal{L} = 10, 50, 100, 500, 1000\ \text{fb}^{-1}$. We consider the process $e^-p \to e^-\gamma^* p \to \nu_e W^- p$. We include the CMS bound.

and luminosity stages of the LHeC and the FCC-he the measurements on $\Delta\kappa_\gamma$ and λ_γ are accessible.

In tables 2–5, we present the sensitivities on the anomalous $\Delta\kappa_\gamma$ and λ_γ couplings through the process $e^-p \to e^-\gamma^* p \to \nu_e W^- p$ at the LHeC and the FCC-he including the systematic uncertainties of δ_{sys}=0%, 1%, 5%, 10% [30, 31], unpolarized and polarized electron beams and with leptonic and hadronic decays of the W-boson.

Estimations of the one-parameter limits on the anomalous $\Delta\kappa_\gamma$ and λ_γ couplings given in equations (8) and (9) are presented in table 2, where one of the anomalous couplings is fixed to zero. In table 2, we consider the leptonic and hadronic decay channels of the process $e^-p \to e^-\gamma^* p \to \nu_e W^- p$ at the LHeC with $\sqrt{s} = 1.30, 1.98$ TeV and integrated luminosities $\mathcal{L} = 10, 30, 50, 70, 100\ \text{fb}^{-1}$. A similar estimation for the anomalous couplings $\Delta\kappa_\gamma$ and λ_γ is presented in table 3, where in this case $\sqrt{s} = 7.07, 10$ TeV at the FCC-he with integrated luminosities $\mathcal{L} = 100, 300, 500, 700, 1000\ \text{fb}^{-1}$, respectively. From these tables, it is clear that in the leptonic channel the limits on the $\Delta\kappa_\gamma$ and λ_γ are of the order of magnitude of few times 10^{-3} to 10^{-2}. However, due to the larger branching ratio, the hadronic channel can improve the constraints by a factor of two or three with respect to the leptonic channel.

From table 3, our best limits for the anomalous couplings $\Delta\kappa_\gamma$ and λ_γ at the FCC-he are the following.

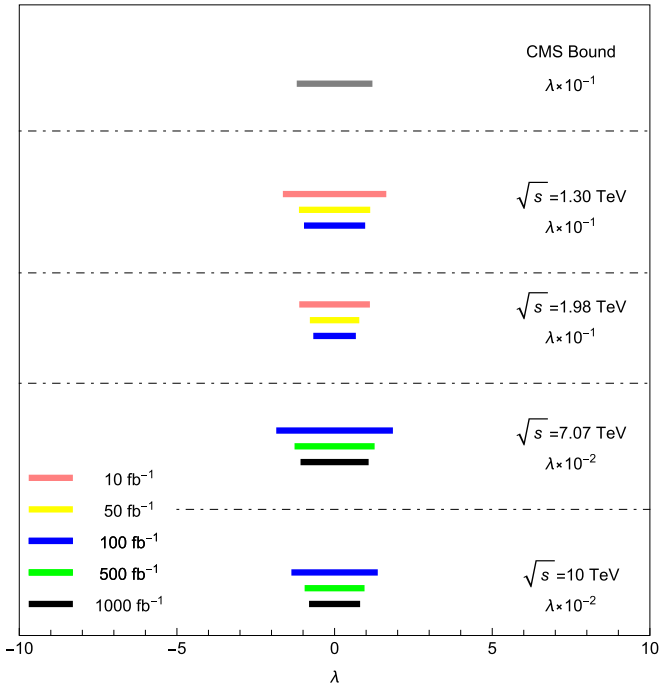

Figure 6. Same as in figure 5, but for λ_γ.

(i) Limits on $\Delta\kappa_\gamma$ and λ_γ for $\sqrt{s} = 7.07$ TeV, $\mathcal{L} = 1000$ fb^{-1} and $P_{e^-} = 0\%$:

$$\Delta\kappa_\gamma = \begin{array}{l} |0.0033|, \quad 95\% \text{ C.L., leptonic,} \\ |0.0019|, \quad 95\% \text{ C.L., hadronic,} \end{array} \tag{21}$$

$$\lambda_\gamma = \begin{array}{l} |0.0098|, \quad 95\% \text{ C.L., leptonic,} \\ |0.0073|, \quad 95\% \text{ C.L., hadronic.} \end{array} \tag{22}$$

(ii) Limits on $\Delta\kappa_\gamma$ and λ_γ for $\sqrt{s} = 10$ TeV, $\mathcal{L} = 1000$ fb^{-1} and $P_{e^-} = 0\%$:

$$\Delta\kappa_\gamma = \begin{array}{l} |0.0031|, \quad 95\% \text{ C.L., leptonic,} \\ |0.0017|, \quad 95\% \text{ C.L., hadronic,} \end{array} \tag{23}$$

$$\lambda_\gamma = \begin{array}{l} |0.0071|, \quad 95\% \text{ C.L., leptonic,} \\ |0.0053|, \quad 95\% \text{ C.L., hadronic.} \end{array} \tag{24}$$

The limits given in equations (21)–(24) are consistent with the corresponding ones of table 1 for the anomalous couplings $\Delta\kappa_\gamma$ and λ_γ.

3.3. Impact of the polarized electron beam on the cross-section of the process $e^-p \to e^-\gamma^* p \to \nu_e W^- p$ at the LHeC and the FCC-he

In the previous sub-sections, the results for the cross-section of the process $e^-p \to e^-\gamma^* p \to \nu_e W^- p$, as well as of the anomalous parameters $\Delta\kappa_\gamma$ and λ_γ are presented

Table 2. Estimations of the 95% C.L. prospects for the anomalous couplings $\Delta\kappa_\gamma$ and λ_γ in the leptonic and hadronic decay channels of the process $e^-p \to e^-\gamma^* p \to \nu_e W^- p$ at the LHeC with $\sqrt{s} = 1.30$, 1.98 TeV and integrated luminosities of $\mathcal{L} = 10$, 30, 50, 70, 100 fb^{-1}. All the limits for $\Delta\kappa_\gamma(\lambda_\gamma)$ are obtained while the other coupling is fixed to their SM value of zero.

95% C.L.		$\sqrt{s} = 1.30$ TeV		$\sqrt{s} = 1.98$ TeV	
		$\delta_{\rm sys} = 0\%$			
Parameter	$\mathcal{L}$ (fb^{-1})	Leptonic channel	Hadronic channel	Leptonic channel	Hadronic channel
$\Delta\kappa_\gamma$	10	[−0.0607, 0.0571]	[−0.0336, 0.0325]	[−0.0499, 0.0473]	[−0.0277, 0.0269]
	30	[−0.0345, 0.0333]	[−0.0192, 0.0189]	[−0.0285, 0.0276]	[−0.0159, 0.0156]
	50	[−0.0266, 0.0259]	[−0.0149, 0.0146]	[−0.0220, 0.0214]	[−0.0123, 0.0121]
	70	[−0.0224, 0.0219]	[−0.0125, 0.0124]	[−0.0185, 0.0181]	[−0.0103, 0.0102]
	100	[−0.0187, 0.0184]	[−0.0105, 0.0104]	[−0.0155, 0.0152]	[−0.0086, 0.0086]
λ_γ	10	[−0.1546, 0.1546]	[−0.1159, 0.1159]	[−0.1022, 0.1022]	[−0.0766, 0.0766]
	30	[−0.1175, 0.1175]	[−0.0881, 0.0881]	[−0.0777, 0.0777]	[−0.0582, 0.0582]
	50	[−0.1034, 0.1034]	[−0.0775, 0.0775]	[−0.0684, 0.0684]	[−0.0512, 0.0512]
	70	[−0.0950, 0.0950]	[−0.0712, 0.0712]	[−0.0628, 0.0628]	[−0.0471, 0.0471]
	100	[−0.0869, 0.0869]	[−0.0652, 0.0652]	[−0.0575, 0.0575]	[−0.0431, 0.0431]
		$\delta_{\rm sys} = 1\%$			
$\Delta\kappa_\gamma$	100	[−0.0260, 0.0253]	[−0.0208, 0.0203]	[−0.0240, 0.0233]	[−0.0203, 0.0198]
λ_γ	100	[−0.1022, 0.1022]	[−0.0914, 0.0914]	[−0.0714, 0.0715]	[−0.0656, 0.0657]
		$\delta_{\rm sys} = 5\%$			
$\Delta\kappa_\gamma$	100	[−0.0953, 0.0867]	[−0.0938, 0.0855]	[−0.0971, 0.0877]	[−0.0961, 0.0869]
λ_γ	100	[−0.1919, 0.1919]	[−0.1905, 0.1905]	[−0.1405, 0.1406]	[−0.1398, 0.1399]
		$\delta_{\rm sys} = 10\%$			
$\Delta\kappa_\gamma$	100	[−0.1988, 0.1643]	[−0.1980, 0.1637]	[−0.2050, 0.1666]	[0.2044, 0.1662]
λ_γ	100	[−0.2692, 0.2692]	[−0.2687, 0.2687]	[−0.1977, 0.1977]	[−0.1974, 0.1975]

Table 3. Estimations of the 95% C.L. prospects for the anomalous couplings $\Delta\kappa_\gamma$ and λ_γ in the leptonic and hadronic decay channels of the process $e^-p \to e^-\gamma^* p \to \nu_e W^- p$ at the FCC-he with $\sqrt{s} = 7.07$, 10 TeV and integrated luminosities of $\mathcal{L} = 100$, 300, 500, 700, 1000 fb^{-1}. All the limits for $\Delta\kappa_\gamma(\lambda_\gamma)$ are obtained while the other coupling is fixed to their SM value of zero.

95% C.L.		$\sqrt{s} = 7.07$ TeV		$\sqrt{s} = 10$ TeV	
		$\delta_{\rm sys} = 0\%$			
Parameter	$\mathcal{L}$ (fb^{-1})	Leptonic channel	Hadronic channel	Leptonic channel	Hadronic channel
$\Delta\kappa_\gamma$	100	[−0.0107, 0.0106]	[−0.0059, 0.0059]	[−0.0100, 0.0099]	[−0.0055, 0.0055]
	300	[−0.0061, 0.0061]	[−0.0034, 0.0034]	[−0.0057, 0.0057]	[−0.0032, 0.0032]
	500	[−0.0047, 0.0047]	[−0.0026, 0.0026]	[−0.0044, 0.0044]	[−0.0025, 0.0025]
	700	[−0.0040, 0.0040]	[−0.0022, 0.0022]	[−0.0037, 0.0037]	[−0.0021, 0.0021]
	1000	[−0.0033, 0.0033]	[−0.0019, 0.0019]	[−0.0031, 0.0031]	[−0.0017, 0.0017]
λ_γ	100	[−0.0175, 0.0175]	[−0.0131, 0.0131]	[−0.0127, 0.0127]	[−0.0095, 0.0095]
	300	[−0.0133, 0.0133]	[−0.0099, 0.0099]	[−0.0096, 0.0096]	[−0.0072, 0.0072]
	500	[−0.0117, 0.0117]	[−0.0088, 0.0088]	[−0.0085, 0.0085]	[−0.0063, 0.0063]
	700	[−0.0107, 0.0107]	[−0.0080, 0.0080]	[−0.0078, 0.0078]	[−0.0058, 0.0058]
	1000	[−0.0098, 0.0098]	[−0.0073, 0.0073]	[−0.0071, 0.0071]	[−0.0053, 0.0053]
		$\delta_{\rm sys} = 1\%$			
$\Delta\kappa_\gamma$	1000	[−0.0193, 0.0188]	[−0.0192, 0.0186]	[−0.0216, 0.0210]	[−0.0199, 0.0194]
λ_γ	1000	[−0.0234, 0.0234]	[−0.0233, 0.0233]	[−0.0176, 0.0176]	[−0.0175, 0.0175]
		$\delta_{\rm sys} = 5\%$			
$\Delta\kappa_\gamma$	1000	[−0.1007, 0.1088]	[−0.1006, 0.1088]	[−0.1022, 0.0892]	[−0.1018, 0.0889]
λ_γ	1000	[−0.0519, 0.0519]	[−0.0519, 0.0519]	[−0.0391, 0.0391]	[−0.0391, 0.0391]
		$\delta_{\rm sys} = 10\%$			
$\Delta\kappa_\gamma$	1000	[−0.2200, 0.1689]	[−0.2200, 0.1689]	[−0.2245, 0.1689]	[−0.2243, 0.1687]
λ_γ	1000	[−0.0735, 0.0735]	[−0.0735, 0.0735]	[−0.0553, 0.0553]	[−0.0553, 0.0553]

Table 4. Estimations of the 95% C.L. prospects for the anomalous couplings $\Delta\kappa_\gamma$ and λ_γ in the leptonic and hadronic decay channels of the process $e^-p \to e^-\gamma^* p \to \nu_e W^- p$ at the LHeC with $\sqrt{s} = 1.30$, 1.98 TeV and integrated luminosities of $\mathcal{L} = 10$, 30, 50, 70, 100 fb^{-1}. All the limits for $\Delta\kappa_\gamma(\lambda_\gamma)$ are obtained while the other coupling is fixed to their SM value of zero. We considered polarized electron beam with $P_e = -80\%$.

95% C.L.		$\sqrt{s} = 1.30$ TeV		$\sqrt{s} = 1.98$ TeV	
		$\delta_{\text{sys}} = 0\%$			
Parameter	$\mathcal{L}$ (fb^{-1})	Leptonic channel	Hadronic channel	Leptonic channel	Hadronic channel
$\Delta\kappa_\gamma$	10	[−0.0449, 0.0429]	[−0.0249, 0.0243]	[−0.0369, 0.0355]	[−0.0205, 0.0201]
	30	[−0.0256, 0.0250]	[−0.0143, 0.0141]	[−0.0211, 0.0206]	[−0.0118, 0.0117]
	50	[−0.0198, 0.0194]	[−0.0110, 0.0109]	[−0.0163, 0.0160]	[−0.0091, 0.0090]
	70	[−0.0167, 0.0164]	[−0.0093, 0.0092]	[−0.0137, 0.0135]	[−0.0076, 0.0076]
	100	[−0.0139, 0.0138]	[−0.0078, 0.0077]	[−0.0113, 0.0113]	[−0.0064, 0.0064]
λ_γ	10	[−0.1335, 0.1335]	[−0.1001, 0.1001]	[−0.0882, 0.0882]	[−0.0661, 0.0661]
	30	[−0.1014, 0.1014]	[−0.0760, 0.0760]	[−0.0670, 0.0670]	[−0.0502, 0.0502]
	50	[−0.0892, 0.0892]	[−0.0669, 0.0669]	[−0.0590, 0.0590]	[−0.0442, 0.0442]
	70	[−0.0820, 0.0820]	[−0.0615, 0.0615]	[−0.0542, 0.0542]	[−0.0406, 0.0406]
	100	[−0.0750, 0.0750]	[−0.0562, 0.0562]	[−0.0496, 0.0496]	[−0.0372, 0.0372]
		$\delta_{\text{sys}} = 1\%$			
$\Delta\kappa_\gamma$	100	[−0.0227, 0.0222]	[−0.0195, 0.0191]	[−0.0216, 0.0211]	[−0.0194, 0.0190]
λ_γ	100	[−0.0956, 0.0956]	[−0.0887, 0.0887]	[−0.0678, 0.0678]	[−0.0643, 0.0643]
		$\delta_{\text{sys}} = 5\%$			
$\Delta\kappa_\gamma$	100	[−0.0943, 0.0859]	[−0.0935, 0.0852]	[−0.0964, 0.0871]	[−0.0958, 0.0866]
λ_γ	100	[−0.1910, 0.1910]	[−0.1902, 0.1902]	[−0.1401, 0.1401]	[−0.1397, 0.1397]
		$\delta_{\text{sys}} = 10\%$			
$\Delta\kappa_\gamma$	100	[−0.1983, 0.1639]	[−0.1978, 0.1636]	[−0.2045, 0.1663]	[0.2042, 0.1661]
λ_γ	100	[−0.2686, 0.2686]	[−0.2687, 0.2687]	[−0.1975, 0.1975]	[−0.1974, 0.1974]

Table 5. Estimations of the 95% C.L. prospects for the anomalous couplings $\Delta\kappa_\gamma$ and λ_γ in the leptonic and hadronic decay channels of the process $e^-p \to e^-\gamma^* p \to \nu_e W^- p$ at the FCC-he with $\sqrt{s} = 7.07$, 10 TeV and integrated luminosities of $\mathcal{L} = 100$, 300, 500, 700, 1000 fb^{-1}. All the limits for $\Delta\kappa_\gamma(\lambda_\gamma)$ are obtained while the other coupling is fixed to their SM value of zero. We considered polarized electron beam with $P_e = -80\%$.

95% C.L.		$\sqrt{s} = 7.07$ TeV		$\sqrt{s} = 10$ TeV	
		$\delta_{\rm sys} = 0\%$			
Parameter	$\mathcal{L}$ (fb^{-1})	Leptonic channel	Hadronic channel	Leptonic channel	Hadronic channel
$\Delta\kappa_\gamma$	100	[−0.0080, 0.0079]	[−0.0044, 0.0044]	[−0.0074, 0.0074]	[−0.0041, 0.0041]
	300	[−0.0045, 0.0045]	[−0.0025, 0.0025]	[−0.0042, 0.0042]	[−0.0024, 0.0024]
	500	[−0.0035, 0.0035]	[−0.0020, 0.0020]	[−0.0033, 0.0033]	[−0.0018, 0.0018]
	700	[−0.0030, 0.0030]	[−0.0016, 0.0016]	[−0.0028, 0.0028]	[−0.0015, 0.0015]
	1000	[−0.0025, 0.0025]	[−0.0014, 0.0014]	[−0.0023, 0.0023]	[−0.0013, 0.0013]
λ_γ	100	[−0.0151, 0.0151]	[−0.0113, 0.0113]	[−0.0110, 0.0110]	[−0.0082, 0.0082]
	300	[−0.0115, 0.0115]	[−0.0086, 0.0086]	[−0.0083, 0.0083]	[−0.0062, 0.0062]
	500	[−0.0101, 0.0101]	[−0.0075, 0.0075]	[−0.0073, 0.0073]	[−0.0055, 0.0055]
	700	[−0.0093, 0.0093]	[−0.0069, 0.0069]	[−0.0067, 0.0067]	[−0.0050, 0.0050]
	1000	[−0.0085, 0.0085]	[−0.0063, 0.0063]	[−0.0061, 0.0061]	[−0.0046, 0.0046]
		$\delta_{\rm sys} = 1\%$			
$\Delta\kappa_\gamma$	1000	[−0.0192, 0.0187]	[−0.0190, 0.0186]	[−0.0192, 0.0187]	[−0.0191, 0.0186]
λ_γ	1000	[−0.0233, 0.0233]	[−0.0232, 0.0232]	[−0.0175, 0.0175]	[−0.0175, 0.0175]
		$\delta_{\rm sys} = 5\%$			
$\Delta\kappa_\gamma$	1000	[−0.1007, 0.0886]	[−0.1007, 0.0886]	[−0.1017, 0.0888]	[−0.1016, 0.0887]
λ_γ	1000	[−0.0519, 0.0519]	[−0.0519, 0.0519]	[−0.0391, 0.0391]	[−0.0391, 0.0391]
		$\delta_{\rm sys} = 10\%$			
$\Delta\kappa_\gamma$	1000	[−0.2204, 0.1687]	[−0.2204, 0.1687]	[−0.2244, 0.1686]	[−0.2243, 0.1685]
λ_γ	1000	[−0.0734, 0.0734]	[−0.0734, 0.0734]	[−0.0553, 0.0553]	[−0.0553, 0.0553]

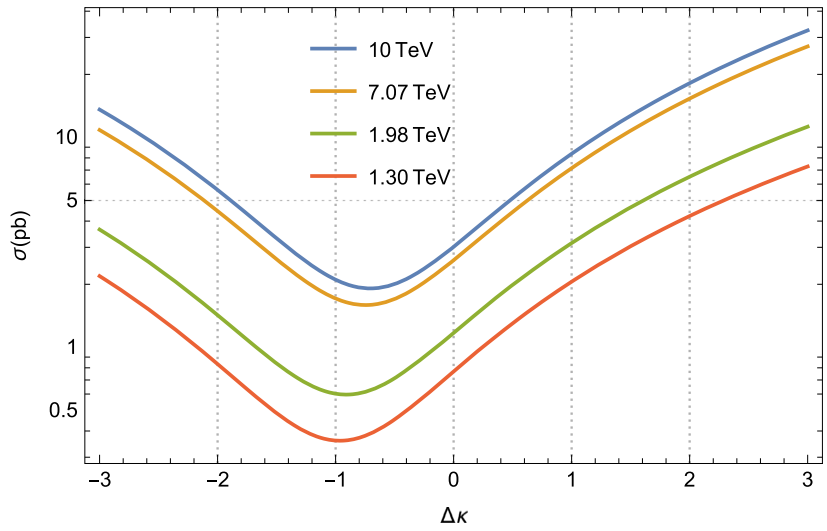

Figure 7. Same as in figure 3, but with polarized electron beam.

with unpolarized electron beam. In this sub-section we discuss the impact of the polarized electron beam in the cross-section and in the anomalous parameters of the aforementioned process.

It is worth noting that a polarized electron beam provides a method to investigate the SM and to diagnose new physics BSM. Proper selection of the electron beam polarization may, therefore be used to enhance the new physics signal and also to considerably suppress backgrounds. We select beam polarization as $P_{e^-} = -80\%$ to enhance our physical process. In addition, as we already mentioned in subsection A, the chiral nature of the weak coupling to fermions results in significant possible enhancements in $\nu_e W^-$ production, as indicated in figures 7 and 8.

Our results for joint variation of the cross-section with the $\Delta\kappa_\gamma$ or λ_γ couplings are shown in figures 7 and 8. In each case, we consider the four center-of-mass energies stages of the FCC-he with their respective integrated luminosities.

The $\sigma(e^-p \to e^-\gamma^* p \to \nu_e W^- p)$ curves as a function of each of the anomalous couplings, setting the other to its SM value of zero, is shown in figures 7 and 8. In this case we consider polarized electron beam with $P_{e^-} = -80\%$. The following results for the cross-section of the process $\sigma(e^-p \to e^-\gamma^* p \to \nu_e W^- p)$ are obtained: $\sigma(\sqrt{s}, \Delta\kappa_\gamma) = 30$ pb for $-3 \leqslant \Delta\kappa_\gamma \leqslant 3$ and $\sigma(\sqrt{s}, \lambda_\gamma) = 10$ pb for $-2 \leqslant \Delta\kappa_\gamma \leqslant 2$, in both cases with $\sqrt{s} = 10$ TeV. From these figures a difference of a factor of 4–10 for the minimum and maximum center-of-mass energies of $1.30-10$ TeV is obtained.

3.4. Impact of the polarized electron beam on the limits of the anomalous couplings $\Delta\kappa_\gamma$ and λ_γ at the LHeC and the FCC-he

In this sub-section, we presented a model-independent global fit on the anomalous couplings $\Delta\kappa_\gamma$ and λ_γ. To carry out this, we made use of the total cross-section for the process $e^-p \to e^-\gamma^* p \to \nu_e W^- p$ in e^-p collisions. The results of the fit for the four FCC-he energy stages with their respective luminosities are shown in figures 9 and 10.

Figures 9 and 10 show the summary plot illustrating the limits that can be obtained of the process $e^-p \to e^-\gamma^* p \to \nu_e W^- p$ on the couplings $\Delta\kappa_\gamma$ and λ_γ. We consider the following

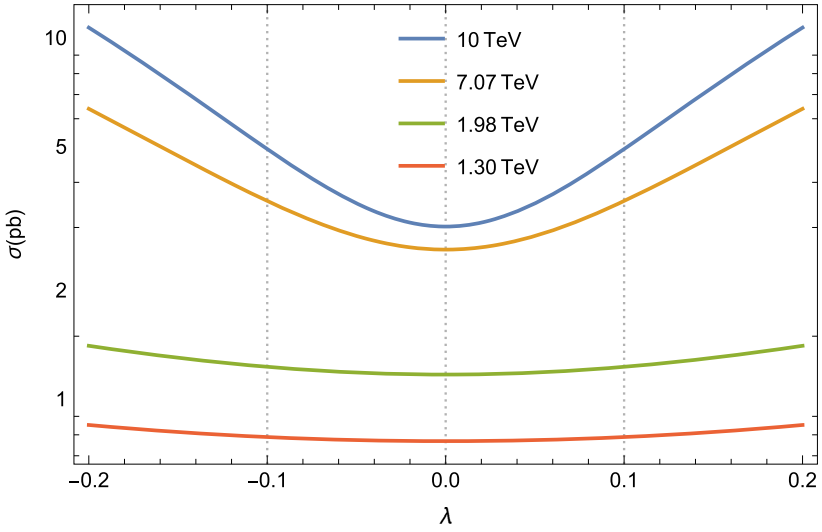

Figure 8. Same as in figure 4, but with polarized electron beam.

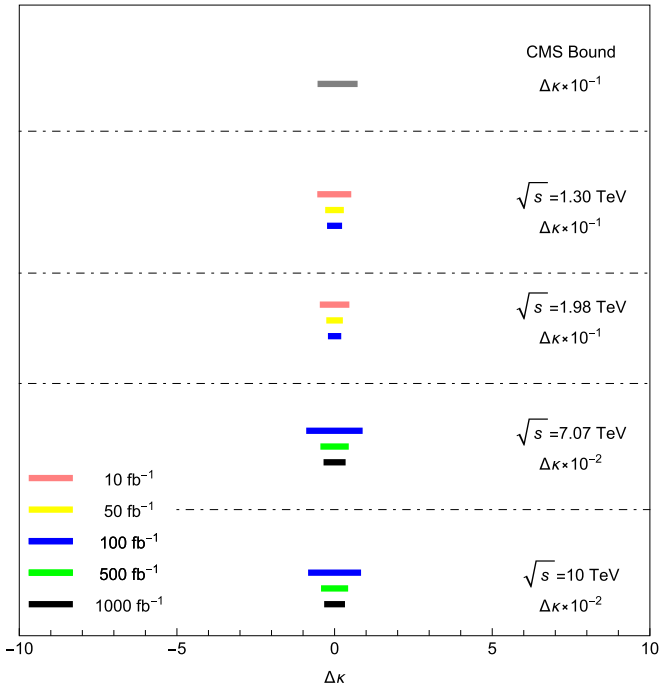

Figure 9. Same as in figure 5, but with polarized electron beam.

center-of-mass energies, luminosities and polarization of the electron beam $\sqrt{s} = 1.30, 1.98, 1.07, 10$ TeV, $\mathcal{L} = 10, 50, 100, 500, 1000$ fb^{-1} and $P_{e^-} = -80\%$, respectively. For comparison, on the same panel we give the constraints from CMS (gray) Collaborations at the LHC.

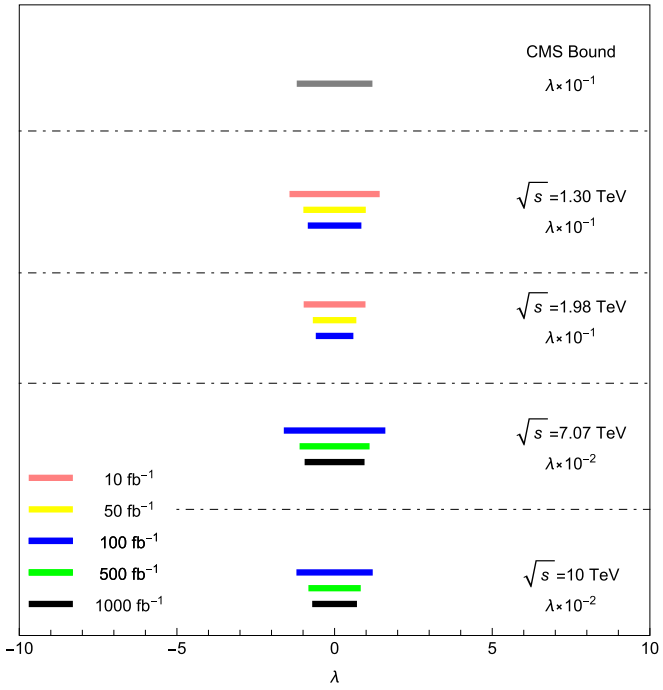

Figure 10. Same as in figure 6, but with polarized electron beam.

To complement our study on the anomalous parameters $\Delta\kappa_\gamma$ and λ_γ through the process $e^-p \to e^-\gamma^* p \to \nu_e W^- p$ with polarized electron beam and considering the parameters of the LHeC and the FCC-he, we give limits for the anomalous couplings of the W^--boson in tables 4 and 5. These limits show the best measurement is compared with the unpolarized case illustrated in tables 2 and 3.

The following limits are set on the couplings $\Delta\kappa_\gamma$ and λ_γ at the FCC-he and with polarized electron beam when one parameter is allowed to vary and the others are set to their SM values of zero.

(i) Limits on $\Delta\kappa_\gamma$ and λ_γ for $\sqrt{s} = 7.07$ TeV, $\mathcal{L} = 1000$ fb^{-1} and $P_{e^-} = -80\%$:

$$\Delta\kappa_\gamma = \begin{array}{l} |0.0025|, \quad 95\%\ \text{C.L., leptonic}, \\ |0.0014|, \quad 95\%\ \text{C.L., hadronic}, \end{array} \tag{25}$$

$$\lambda_\gamma = \begin{array}{l} |0.0085|, \quad 95\%\ \text{C.L., leptonic}, \\ |0.0063|, \quad 95\%\ \text{C.L., hadronic}. \end{array} \tag{26}$$

(ii) Limits on $\Delta\kappa_\gamma$ and λ_γ for $\sqrt{s} = 10$ TeV, $\mathcal{L} = 1000$ fb^{-1} and $P_{e^-} = -80\%$:

$$\Delta\kappa_\gamma = \begin{array}{l} |0.0023|, \quad 95\%\ \text{C.L., leptonic}, \\ |0.0013|, \quad 95\%\ \text{C.L., hadronic}, \end{array} \tag{27}$$

$$\lambda_\gamma = \begin{array}{l} |0.0061|, \quad 95\%\ \text{C.L., leptonic}, \\ |0.0046|, \quad 95\%\ \text{C.L., hadronic}. \end{array} \tag{28}$$

A direct comparison of the results shown in the equations (21)–(24) for the unpolarized case and equations (25)–(28) for the case with polarized electron beam for the anomalous couplings $\Delta\kappa_\gamma$ and λ_γ clearly shows that the polarized electron beam effect translates into a factor of 1.35 in the measurement of $\Delta\kappa_\gamma$ and λ_γ.

An important observation on the bounds for $\Delta\kappa_\gamma$ and λ_γ given in tables 2–5 and that represent the bounds with increasing $\delta_{\rm sys}$ values at the FCC-he are almost unchanged with respect to the values luminosity and for the center-of-mass energy values. The reason for this situation is the $\delta_{\rm st}$ which is much smaller than the $\delta_{\rm sys}$.

On the other hand, it is appropriate to mention that the limits shown in tables 2–5 are competitive with the experimental and phenomenological limits obtained by the ATLAS, CMS, CDF, D0, ALEP, DELPHI, L3 and OPAL Collaborations, as well as by the LHC, HL-LHC and the LHeC which are shown in table 1. However, are weaker by $\mathcal{O}(10^{-2} - 10^{-1})$ orders of magnitude than those of the FCC-he, CEPC, ILC and CLIC.

3.5. Quantitative comparison of various colliders to probing the aTGC $\Delta\kappa_\gamma$ and λ_γ

In this subsection, we present a quantitative comparison of various present and future colliders in context of limit on the aTGC with our results to probe the aTGC $\Delta\kappa_\gamma$ and λ_γ. We compare our results for the aTGC with other ways to probe the anomalous vertex $WW\gamma$ at the future lepton colliders, such as the ILC, CEPC and CLIC, as well as at the LHC, HL-LHC, LHeC and the FCC-he (see table 1). In this regard, the authors of [27], specifically estimated bounds on the anomalous $WW\gamma$ couplings through the processes $e^+e^- \to W^+W^-$, $e^+e^- \to e^+\gamma^*e^-$ and $e^+e^- \to e + \gamma^*\gamma^*e^- \to W^+\gamma^*\gamma^*W^-$ with unpolarized and polarized electron beams at the CLIC. This paper shows that its obtained limits on the anomalous couplings through the above mentioned processes can highly improve the present experimental limits. Its limits obtained for $\Delta\kappa_\gamma$ and λ_γ are of the order of 10^{-3} for the unpolarized case and of 10^{-4} for the polarized case (see tables 2, 3 of [27]). For our case, we consider the process $e^-p \to e^-\gamma^*p \to \nu_e W^-p$ and our best limits are obtained for the FCC-he. We consider $\mathcal{L} = 1\ {\rm ab}^{-1}@\sqrt{s} = 7.07,\ 10$ TeV with unpolarized and polarized electron beam based on future FCC-he data. Our limits for $\Delta\kappa_\gamma$ and λ_γ, might reach up to $\mathcal{O}(10^{-3})$ level in the most ideal with $1\ {\rm ab}^{-1}$ set data and $\delta_{\rm sys} = 0\%$ for the leptonic and hadronic channels, respectively. Although the conditions for the study of the aTGC are different, our results are competitive with those from [27], as well as of the ATLAS, CMS, CDF, DO, ALEP, DELPHI, L3 and OPAL Collaborations, reported in table 1. More recently in [26], using the reactions of single W production and W^+W^- double production, that is to say $e^+e^- \to e^+W^-\nu_e$ and $e^+e^- \to W^+W^-$, it is expected that the sensitivities would be improved at the ILC, due to the larger luminosity, higher energy and polarized electron beams. In [16], a detailed study on the aTGC is carried out through the $e^+e^- \to W^+W^-$ process for the $\sqrt{s} = 240$ GeV and $\mathcal{L} = 5\ {\rm ab}^{-1}$ of the CEPC. With these parameters can collect a total number of 8.6×10^7 events of W pairs, with 45%, 44% and 11% decaying, respectively, in the hadronic, semi-leptonic and leptonic channels. In addition, for their study on the aTGC they use the five kinematical angles in the $e^+e^- \to W^+W^-$ process to constrain the aTGC and relevant dimension-six operators at the CEPC up to the order of magnitude of 10^{-4} at 95% C. L. From the comparison of our study via the $e^-p \to e^-\gamma^*p \to \nu_e W^-p$ process at the LHeC and the FCC-he with respect to the process $e^+e^- \to W^+W^-$ at the CEPC, these last results indicate an improvement in the measurements for the aTGC. Our predictions indicate that the aTGC can be measured more weakly at the LHeC and the FCC-he by an order of magnitude less than in comparison with the predictions of the CEPC. However, better than the ATLAS, CMS, CDF, DO, ALEP, DELPHI, L3 and OPAL Collaborations. Moreover, one of the

advantages of the $\gamma^* p$ collision modes and as a consequence of the processes studied in our paper is that they can isolate $WW\gamma$ couplings from WWZ couplings. Additionally, these processes have a very clean experimental environment, since they have no interference with weak and strong interactions. It is worth mentioning that in our study we consider systematic uncertainties of $\delta_{\rm sys} = 0\%,\ 1\%,\ 5\%,\ 10\%$, while in the case of the processes studied in [16, 26, 27] these are not taken into account. On the other hand, the bounds on the aTGC from $e^- p \to e^- W^{\pm} j$ scattering might reach up to $\mathcal{O}(10^{-3})$ level with the $\mathcal{L} = (2-3)\,\text{ab}^{-1}$ data set at the future LHeC [17] (see table 2). While the constraints on the aTGC of $pp \to W^+W^-$ at the LHC-14 [16] with a luminosity of 300 fb^{-1} and 3000 fb^{-1} are obtained $|\Delta\kappa_\gamma| = 5.8 \times 10^{-3}$, $|\lambda_\gamma| = 1.1 \times 10^{-3}$ and $|\Delta\kappa_\gamma| = 1.4 \times 10^{-2}$, $|\lambda_\gamma| = 3.3 \times 10^{-3}$ (see table 4). Through a comparison of our results with those of LHeC and LHC-14, it is found that our results are competitive, and in some cases our results improve those of LHeC and HL-LHC. On the other hand, it is expected that the unprecedented energy of pp collisions at the HE-LHC will significantly improve sensitivity to the scale of multi-TeV over LHC and HL-LHC. However, the experimental environment is expected to be challenging at the HE-LHC, primarily due to a significant increase of the number of pp collisions. The HE-LHC is planned to be operated at a center-of-mass energy of $\sqrt{s} = 27$ TeV with 800 pile-up collisions at the peak luminosity. Such extreme pile-up conditions are expected to be particularly challenging for identifying hadronically decaying W/Z boson.

With respect to our previous study on the $WW\gamma$ couplings at the CLIC [85], we probe the anomalous parameters $\Delta\kappa_\gamma$ and λ_γ in the collisions $\gamma\gamma$, $\gamma\gamma^*$ and $\gamma^*\gamma^*$ modes, through the $\gamma\gamma \to W^+W^-$, $e^+\gamma \to e^+\gamma^*\gamma \to e^+W^-W^+$ and $e^+e^- \to e^+\gamma^*\gamma^* e^- \to e^+W^-W^+e^-$ signals. Basing our results on futures CLIC data, the bounds for $\Delta\kappa_\gamma$ and λ_γ might reach up to $\mathcal{O}(10^{-5} - 10^{-4})$ level in the most ideal with $5\,\text{ab}^{-1}$ set data. Therefore, our limits on the anomalous couplings $\Delta\kappa_\gamma$ and λ_γ indicate that the CLIC for its three energy stages can measure these couplings to a level of precision that exceeds that of the LHC and HL-LHC, as well as of the CDF, D0, ALEPH, DELPHI, L3, OPAL Collaborations by more than $\mathcal{O}(10^{-3} - 10^{-2})$ order of magnitude. While in the case of LHeC, FCC-he, ILC and CEPC, the CLIC results are exceeded in $\mathcal{O}(10^{-2} - 10^{-1})$ order of magnitude. See table 1 for a comparison of various proposed colliders to probe the aTGC $\Delta\kappa_\gamma$ and λ_γ.

To conclude this subsection, it is worth mentioning that for the FCC-ee, the high luminosity and the excellent energy calibration at the Z, WW, and ZH energies are building blocks of a unique program. In addition, accumulating a larger amount of data, which is designed up to 10 ab^{-1} it is expected that the FCC-ee can improve constraints on the aTGC [86, 87].

4. Conclusions

The production cross-section of the process $e^- p \to e^- \gamma^* p \to \nu_e W^- p$ in the SM is 1.50 pb in the case of unpolarized electron beam and of 3 pb for the case of polarized electron beam with $\sqrt{s} = 10\,\text{TeV}$ as is shown in figures 3, 4 and 7, 8. In addition, one can see the $\sigma(e^- p \to e^- \gamma^* p \to \nu_e W^- p)$ increases monotonically with $\Delta\kappa_\gamma$ and the absolute value of λ_γ within the parameter region allowed by current experiments, this is enough to probe anomalous triple gauge couplings contributions. These couplings could reach $\mathcal{O}(10^{-3})$ when $\sqrt{s} = 10\,\text{TeV}$, $\mathcal{L} = 1000\,\text{fb}^{-1}$ and $\delta_{\rm sys} = 0\%$.

From the results in tables 2–5 and figures 3–10, we could see a significant improvement in the measurement for $\Delta\kappa_\gamma$ and λ_γ compared to the present ATLAS, CMS, CDF, D0, ALEP, DELPHI, L3 and OPAL collaborations bounds (see table 1).

We have presented new searches of anomalous $W^+W^-\gamma$ trilinear gauge boson couplings from $e^-p \to e^-\gamma^*p \to \nu_e W^-p$ channel analyzing $(10 - 1000)$ fb^{-1} of integrated luminosities and center-of-mass energies $\sqrt{s} = 1.30, 1.98, 7.07, 10$ TeV, respectively. We set model-independent limits on anomalous triple gauge couplings $\Delta\kappa_\gamma$ and λ_γ for the final states $\nu_e W^-$ at the 95% C.L.: $\Delta\kappa_\gamma = \pm 0.0017$, $\lambda_\gamma = \pm 0.0053$ (unpolarized electron beam) and $\Delta\kappa_\gamma = \pm 0.0013$, $\lambda_\gamma = \pm 0.0046$ (polarized electron beam) with $\sqrt{s} = 10$ TeV, $\mathcal{L} = 1000$ fb^{-1} and $\delta_{\rm sys} = 0\%$ for both cases. The W^--boson is identified through the hadronic decays channel. In addition, it is worth mentioning that the impact of the polarized electron beam translates into a factor of 1.35 with respect to the non-polarized case (see tables 2–5).

Reference [17] is carried out entirely by using virtual photons as propagators. In our study, the photons entering the main process are considered as quasi-real particles and the EPA approach is used for distributions of photons.

In [18], the main process $e^-p \to e^-\gamma^*p \to e^-W^-q'X$ through the subprocess $\gamma^*p \to W^-q'$ is examined for the anomalous $WW\gamma$ couplings. Here, it is assumed that the photons scattered from electrons interact with the proton and form the subprocess $\gamma^*p \to W^-q'$ (see equations (11)–(19) in [18]). However, in this work, we suppose the main process $e^-p \to e^-\gamma^*p \to \nu_e Wp$ through the subprocess $\gamma^*e^- \to \nu_e W^-$ is investigated to the anomalous $WW\gamma$ couplings. It can be seen from this analysis that the two processes are completely different from each other.

In conclusion, the measurement of the $e^-p \to e^-\gamma^*p \to \nu_e W^-p$ channel at the LHeC and the FCC-he would provide a promising opportunity to probe the anomalous couplings $\Delta\kappa_\gamma$ and λ_γ without the complications of other couplings especially QCD backgrounds, and therefore improve our knowledge of the gauge sector. Furthermore, for future measurement of $\Delta\kappa_\gamma$ and λ_γ, we expect complementary studies with different electron beam polarizations, as well as a more realistic detector-level analysis, will be very useful.

Acknowledgments

AGR and MAHR thank SNI and PROFEXCE (México).

ORCID iDs

A Gutiérrez-Rodríguez https://orcid.org/0000-0003-4431-3159
M Köksal https://orcid.org/0000-0002-7377-9049
A A Billur https://orcid.org/0000-0003-1564-6683

References

[1] Glashow S L 1961 *Nucl. Phys.* **22** 579
[2] Salam A and Ward J C 1964 *Phys. Lett.* **13** 168
[3] Weinberg S 1967 *Phys. Rev. Lett.* **19** 1264
[4] Alitti J *et al* 1992 *Phys. Lett.* B **277** 194
[5] Abe F *et al* 1995 *Phys. Rev. Lett.* **74** 1936
[6] Abachi S *et al* 1995 *Phys. Rev. Lett.* **75** 1034
[7] Abe F *et al* 1995 *Phys. Rev. Lett.* **75** 1023
[8] Abachi S *et al* 1995 *Phys. Rev. Lett.* **75** 1034
[9] Aaltonen T *et al* (CDF Collaboration) 2009 *Phys. Rev. Lett.* **102** 242001
[10] Abazov V M *et al* (D0 Collaboration) 2012 *Phys. Lett.* B **718** 451

[11] Alam M S *et al* 1995 *Phys. Rev. Lett.* **74** 2885
[12] Schael S *et al* (ALEPH, DELPHI, L3, OPAL Collaborations and LEP Electroweak Collaborations) 2013 *Phys. Rep.* **532** 119
[13] Heuer R D 2001 *TESLA Technical Design Report Part III: Physics at an e + e Linear Collider Report No. DESY 2001-011, ECFA 2001-209* ECFA/DESY LC Physics Working Group arXiv: hep-ph/0106315
[14] Aaboud M(ATLAS Collaboration) *et al* 2017 *Eur. Phys. J.* C **77** 563
[15] Sirunyan A M *et al* (CMS Collaboration) 2017 *Phys. Lett.* B **772** 21
[16] Bian L, Shu J and Zhang Y 2015 *J. High Energy Phys.* JHEP09(2015)206
[17] Li R, Shen X-M, Wang K, Xu T, Zhang L and Zhu G 2018 *Phys. Rev.* D **97** 075043
[18] Köksal M, Billur A A, Gutiérrez-Rodríguez A and Hernández-Ruíz M A 2019 arXiv:1910.06747v1 [hep-ph]
[19] Bambade P *et al* 2018 *The International Linear Collider: A Global Project* Report No. DESY 19-037, FERMILAB-FN-1067-PPD, IFIC/19-10, IRFU-19-10, JLAB-PHY-19-2854, KEK Preprint 2018-92, LAL/RT 19-001, PNNL-SA-142168, SLAC-PUB-17412 CERN
[20] Burrows P N *et al* 2018 *The Compact Linear Collider (CLIC)-2018 Summary Report (CERN Yellow Rep.Monogr.)* Report No.CERN-2018-005-M CERN 1-98
[21] Fernandez J L A *et al* (LHeC Study Group) 2012 *J. Phys. G: Nucl. Part. Phys.* **39** 075001
[22] Fernandez J L A *et al* (LHeC Study Group) 2012 arXiv:1211.5102
[23] Fernandez J L A *et al* 2012 arXiv:1211.4831
[24] Brüning O and Klein M 2013 *Mod. Phys. Lett* A **28** 1330011
[25] Brüning O, Jowett J, Klein M, Pellegrini D, Schulte D and Zimmermann F 2017 *Study FCC-he Baseline Parameters Report No. EDMS 17979910 FCC-ACC-RPT-0012,V1.0* CERN https://fcc.web.cern.ch/Documents/FCCheBaselineParameters.pdf
[26] Baer H *et al* 2013 arXiv:1306.6352
[27] Ari V, Billur A A, Inan S C and Köksal M 2016 *Nucl. Phys.* B **906** 211
[28] Bi H-Y, Zhang R-Y, Wu X-G, Ma W-G, Li X-Z and Owusu S 2017 *Phys. Rev.* D **95** 074020
[29] Acar Y C, Akay A N, Beser S, Karadeniz H, Kaya U, Oner B B and Sultansoy S 2017 *Nucl. Inst. Methods Phys. Res.* A **871** 47
[30] Dutta S *et al* 2015 *Eur. Phys. J.* C **75** 577
[31] Armesto N *et al* 2019 *Phys. Rev.* D **100** 074002
[32] Baur U and Zeppenfeld D 1988 *Phys. Lett.* B **201** 383
[33] Hagiwara K, Peccei R D, Zeppenfeld D and Hikasa K 1987 *Nucl. Phys.* B **282** 253
[34] Hagiwara K, Ishihara S, Szalapski R and Zeppenfeld D 1992 *Phys. Lett.* B **283** 353
[35] Diehl M and Nachtmann O 1994 *Z. Phys.* C **62** 397
[36] Sahin I and Billur A A 2011 *Phys. Rev.* D **83** 035011
[37] Cakir I T, Cakir O, Senol A and Tasci A T 2014 *Acta Phys. Pol.* B **45** 1947
[38] Etesami S M *et al* 2016 *Eur. Phys. J.* C **76** 533
[39] Ari V, Billur A A, Inan S C and Köksal M 2016 *Nucl. Phys.* B **906** 211
[40] Atag S and Cakir I T 2001 *Phys. Rev.* D **63** 033004
[41] Atag S and Sahin I 2001 *Phys. Rev.* D **64** 095002
[42] Sahin B 2009 *Phys. Scr.* **79** 065101
[43] Papavassiliou J and Philippides K 1999 *Phys. Rev.* D **60** 113007
[44] Choudhury D, Kalinowski J and Kulesza A 1999 *Phys. Lett.* B **457** 193
[45] Chapon E, Royon C and Kepka O 2010 *Phys. Rev.* D **81** 074003
[46] Ellis J, Ge S-F, He H-J and Xiao R-Q 2019 arXiv:1902.06631
[47] Gaemers K J F and Gournaris G J 1979 *Z. Phys.* C **1** 259
[48] De Rujula A, Gavela M B, Hernandez P and Masso E 1992 *Nucl. Phys.* B **384** 3
[49] Hagiwara K, Ishihara S, Szalapski R and Zeppenfeld D 1993 *Phys. Rev.* D **48** 2182
[50] Ginzburg I F 2015 arXiv:1508.06581
[51] Ginzburg I F, Kotkin G L, Panfil S L, Serbo V G and Telnov V I 1984 *Nucl. Instrum. Methods Phys. Res.* A **219** 5
[52] Brodsky S J, Kinoshita T and Terazawa H 1971 *Phys. Rev.* D **4** 1532
[53] Budnev V M, Ginzburg I F, Meledin G V and Serbo V G 1975 *Phys. Rep.* **15** 181
[54] Terazawa H 1973 *Rev. Mod. Phys.* **45** 615
[55] Yang J M 2005 *Ann. Phys.* **316** 529
[56] Baur G *et al* 2002 *Phys. Rep.* **364** 359
[57] Piotrzkowski K 2001 *Phys. Rev.* D **63** 071502

[58] Abulencia A *et al* (CDF Collaboration) 2007 *Phys. Rev. Lett.* **98** 112001
[59] Aaltonen T *et al* (CDF Collaboration) 2009 *Phys. Rev. Lett.* **102** 222002
[60] Aaltonen T *et al* (CDF Collaboration) 2009 *Phys. Rev. Lett.* **102** 242001
[61] Chatrchyan S *et al* (CMS Collaboration) 2012 *J. High Energy Phys.* JHEP01(2012)052
[62] Chatrchyan S *et al* (CMS Collaboration) 2012 *J. High Energy Phys.* JHEP11(2012)080
[63] Abazov V M *et al* (D0 Collaboration) 2013 *Phys. Rev.* D **88** 012005
[64] Chatrchyan S *et al* (CMS Collaboration) 2013 *J. High Energy Phys.* JHEP07(2013)116
[65] Inan S C 2010 *Phys. Rev.* D **81** 115002
[66] Inan S C 2015 *Nucl. Phys.* B **897** 289
[67] Inan S C 2011 *Int. J. Mod. Phys.* A **26** 3605
[68] Sahin I and Inan S C 2009 *J. High Energy Phys.* JHEP09(2009)069
[69] Atag S, Inan S C and Sahin I 2010 *J. High Energy Phys.* JHEP09(2010)042
[70] Sahin I and Sahin B 2012 *Phys. Rev.* D **86** 115001
[71] Sahin B and Billur A A 2012 *Phys. Rev.* D **86** 074026
[72] Senol A 2014 *Int. J. Mod. Phys.* A **29** 1450148
[73] Senol A 2013 *Phys. Rev.* D **87** 073003
[74] Fichet S, von Gersdorff G, Lenzi B, Royon C and Saimpert M 2015 *J. High Energy Phys.* JHEP02 (2015)165
[75] Sun H 2014 *Phys. Rev.* D **90** 035018
[76] Sun H 2014 *Nucl. Phys.* B **886** 691
[77] Sun H, Zhou Y J and Hou H S 2015 *J. High Energy Phys.* JHEP02(2015)064
[78] Senol A and Köksal M 2015 *J. High Energy Phys.* JHEP03(2015)139
[79] Wang X J, Sun H and Luo X 2017 *Adv. High Energy Phys.* **2017** 4693213
[80] Belyaev A, Christensen N D and Pukhov A 2013 *Comput. Phys. Commun.* **184** 1729
[81] Hernández-Ruíz M A, Gutiérrez-Rodríguez A, Köksal M and Billur A A 2019 *Nucl. Phys.* B **941** 646
[82] Köksal M, Billur A A, Gutiérrez-Rodríguez A and Hernández-Ruíz M A 2019 *Int. J. Mod. Phys.* A **34** 1950076
[83] Gutiérrez-Rodríguez A, Hernández-Ruíz M A, Köksal M and Billur A A 2019 arXiv:1903.04135
[84] Köksal M, Billur A A, Gutiérrez-Rodríguez A and Hernández-Ruíz M A 2019 arXiv:1905.02564
[85] Billur A A, Köksal M, Gutiérrez-Rodríguez A and Hernández-Ruíz M A 2019 arXiv:1909.10299
[86] Bicer M *et al* (TLEP Design Study Working Group collaboration) 2014 *J. High Energy Phys.* JHEP01(2014)164
[87] Marzocca D 2014 arXiv:1405.3841